energies

MDPI

Article

Development of Intelligent Genetic Optimization Algorithm for Fluid–Thermal Interaction in Machinery Engine Cooling Systems

Jiwei Zhang [1,2], Xinze Song [1], Wenbin Yu [1,*] and Feiyang Zhao [1]

[1] School of Energy and Power Engineering, Shandong University, Jinan 250100, China; zhangjiwei1@lovol.com (J.Z.); 202314523@mail.sdu.edu.cn (X.S.); fyzhao@sdu.edu.cn (F.Z.)
[2] Weichai Lovol Intelligent Agricultural Technology Co., Ltd., Weifang 261206, China
* Correspondence: wbyu@sdu.edu.cn

Abstract

With advancements in simulation technology, fluid–thermal interaction (FTI) has become a vital tool in machinery powertrain development. Traditional engine cooling systems, with mechanically coupled components like water pumps and fans, lack adaptive cooling control. Electronic cooling systems, however, use variable-speed components to enhance performance. Combining FTI simulations with intelligent optimization algorithms offers a novel approach to designing control strategies for these systems. This study establishes a multi-objective optimization model for pump and fan speed control in electronic cooling systems. Using MATLAB/Simulink 2018 and Fluent 2022R1, co-simulations were performed, and an elite-strategy-based NSGA-II algorithm was implemented. Different weights were assigned to optimization objectives based on engine performance requirements. The results provide fitted functions for heat exchange capacity and cylinder liner temperature versus flow rates, along with optimal solutions for a 65 kW engine under three weight configurations. These findings support control strategy design and demonstrate the integration of FTI with genetic algorithms.

Keywords: cooling system; fluid–structure interaction; co-simulation; optimization algorithm

1. Introduction

With the advancement of engine technology, significant improvements have been achieved in fuel economy and power performance. The overall development focus has shifted toward lightweight design, with component weight reduction emerging as a primary trend in contemporary engine development [1,2]. However, higher power density implies that critical engine components may encounter thermal overload-related issues, necessitating more efficient and rational thermal management for high-power, high-speed engines [3,4].

As an essential subsystem, the cooling system ensures the engine maintains appropriate operating temperatures across all working conditions, thereby guaranteeing operational reliability. Traditional powertrain cooling systems employ mechanical coupling between the engine crankshaft and components like water pumps and fans. Consequently, the rotational speeds of these components become unilaterally proportional to engine speed, preventing adaptive regulation based on actual thermal demands. This limitation frequently leads to insufficient cooling efficiency or excessive cooling [5].

In the context of increasing component intelligence, modern engine electronic cooling systems—comprising electric water pumps, electric fans, and electronic thermostats—demonstrate substantial potential for ensuring cooling effectiveness in high-power engines.

Check for updates

Academic Editor: Francesco Nocera

Received: 17 December 2025
Revised: 8 January 2026
Accepted: 14 January 2026
Published: 16 January 2026

Copyright: © 2026 by the authors. Licensee MDPI, Basel, Switzerland. This article is an open access article distributed under the terms and conditions of the Creative Commons Attribution (CC BY) license.

These systems autonomously adjust component speeds via control strategies tailored to real-time thermal load conditions [6,7]. During engine startup or low-load operation, the electronic cooling system operates pumps and fans at reduced speeds to prevent performance degradation from overcooling. Conversely, under high-load conditions, it elevates rotational speeds to enhance cooling capacity, thereby safeguarding operational reliability.

Research and optimization of electronic cooling systems began early, with the concept of electric fans introduced as early as the 1980s, replacing traditional mechanical fans. In 2005, BMW pioneered the use of electric water pumps in vehicles, reducing energy consumption and improving cooling efficiency. Studies on electronic cooling systems primarily focus on component performance improvements and control strategy optimization. Elena Cortona demonstrated that electric water pumps consume only a quarter of the energy of traditional mechanical pumps, significantly enhancing engine efficiency [8]. Osman Keith A et al. [9] applied genetic algorithms for multi-objective optimization of cooling pumps, improving their efficiency. In 2017, the University of Malta proposed a continuously variable speed control strategy for electric fans in racing engines, validated through MATLAB/Simulink simulations, showing improved engine efficiency. John R. Wagner et al. used vehicle ECUs to control electronic thermostats, demonstrating advantages such as faster response and reduced secondary pollution compared to traditional thermostats [10]. Recent advances in thermal management have demonstrated the efficacy of combining numerical simulation with intelligent optimization algorithms. Wang et al. combined CFD simulation with multi-objective optimization to study microchannel cooling under fixed area constraints. They found that optimized zigzag structures significantly improve thermal performance while reducing flow resistance, providing a practical design approach for high-heat-flux electronics [11]. Jamali et al. proposed a novel γ-parameter strategy for thermoelectric cooler optimization, shifting focus from temperature control to minimizing entropy generation. By dynamically tuning electrical current, their approach enables near-optimum performance at all times [12].

With the development of computer simulation technology, fluid–thermal interaction (FTI) has become a powerful tool in engineering design [13–15]. For engine cooling systems, FTI-based CFD simulations enable multi-physics analysis of coolant flow and heat transfer, reducing material and experimental costs compared to traditional testing [16]. Recent studies include Nageswara et al., who used FLUENT 6.0 to analyze axial fan flow characteristics in engine cooling systems, showing that adding fixed rings to fan tips can improve efficiency by preventing casing reflux [17]. Zeng et al. proposed a CFD and data-driven optimization framework for battery cooling systems, demonstrating potential improvements in coolant performance, battery lifespan, and safety [18].

Compared to 3D numerical simulations, zero-dimensional/one-dimensional (0D/1D) simulations, despite providing fewer details, offer strong capabilities in replicating the macroscopic behavior of systems, making them a valuable tool for studying powertrain cooling systems. Park et al. [19] developed a heat transfer model for powertrain cooling systems, creating simulation programs for system analysis and heat exchanger performance evaluation, providing significant reference values. Adsul et al. [20] used 1D simulation methods with GT-Suite to analyze flow and temperature distribution in a six-cylinder diesel engine's cooling system, reducing the need for prototype testing. Qiu et al. [21] employed Pro/Engineer for 3D modeling of a diesel engine's water jacket and GT-COOL for 1D simulation of the overall cooling process, obtaining data on flow, temperature, and pressure. They then used ANSYS CFX for 3D simulation of the worst-performing cylinder, optimizing the cooling system design through 1D/3D co-simulation.

Intelligent cooling systems, featuring electric water pumps and fans, require optimization of multiple parameters to ensure efficient operation. However, these parameters

often conflict. For example, increasing pump flow and fan speed enhances cooling but may reduce engine thermal efficiency by dissipating excessive heat. Genetic algorithms (GA) evaluate individual solutions using fitness functions, simulating natural selection. Individuals are encoded in binary, and iterative optimization is performed [22–24]. Srinivas et al. [25] introduced the non-dominated sorting genetic algorithm (NSGA), and Deb et al. [26] enhanced it with an elite strategy, improving population diversity, convergence speed, and computational efficiency [27]. Li et al. [28] applied GA for dual-objective optimization of coolant flow in engine cooling systems, reducing power consumption within specified flow ranges.

As mentioned above, for intelligent engine cooling systems using electric water pumps and fans, coordinating the speeds of these components to balance cooling efficiency and thermal efficiency is crucial. This study establishes a 1D-3D co-simulation method for powertrain engine cooling systems based on CFD fluid–thermal interaction (FTI) and MATLAB/Simulink 2018. Using NSGA-II, the results were optimized to determine the optimal combination of water pump flow rate and air flow velocity for each operating condition within a specified engine power range. This approach provides a methodological reference for designing intelligent cooling systems.

2. Simulink Model

2.1. Simulink Cooling System

In order to better reproduce the process of fluid flow and heat transfer in various components of the powertrain cooling system, this study adopted the Thermal Liquid module package in Simulink. This module package includes basic components such as water pumps, fans, pipes, and thermostats, and the working flow rate of the components can be adjusted. A one-dimensional simulation model was built, incorporating various important components of the powertrain engine radiator, as shown in Figure 1. The one-dimensional model mainly consists of the pump module, radiator module, engine module, thermostat module, pipe module, expansion tank module, as well as several temperature and pressure sensor modules and display modules. Among them, the engine module is a subsystem composed of several modules, mainly including the thermal mass module and the pipe module. The overall system composition is shown in Figure 1. By changing the heat input to the engine module to simulate changes in engine power, the aim is to observe the variation patterns of cooling water temperature in different parts of the system, while also providing initial conditions for three-dimensional simulations.

2.2. System Modules

A fixed-displacement water pump module was used to simulate an electronically controlled water pump with adjustable speed, as shown in Figure 2. The pump speed was dynamically adjusted in real-time by modifying the rotation parameter in the MATLAB workspace.

The heat exchanger was simulated using a Heat Exchanger module combined with a Controlled Temperature Source module shown in Figure 3. The Heat Exchanger module models heat transfer between two fluids through pipes, where the A1 and B1 ports represent the hot fluid inlet and outlet, respectively, the H2 port corresponds to the incoming temperature of the external fluid (air), the C2 port represents the air heat capacity flow rate, and the HC2 port corresponds to the external air convective heat transfer coefficient.

To simulate heat exchange within the engine, an engine subsystem was constructed using a thermal mass module, a water jacket module, and a pipe module, as shown in Figure 4. The thermal mass module simulates the temperature rise process of the water

jacket when heated, calculates the wall temperature as it absorbs heat, and assigns this temperature to the wall temperature input port of the cooling water jacket.

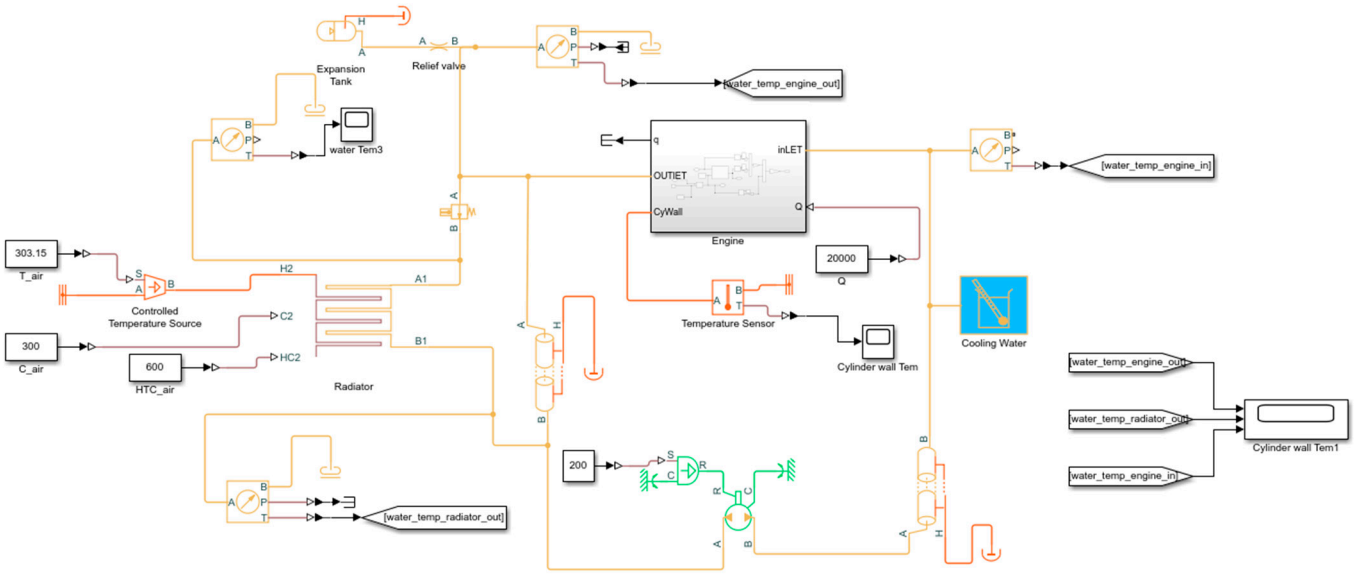


Figure 1. Simulink model of the powertrain engine cooling system.

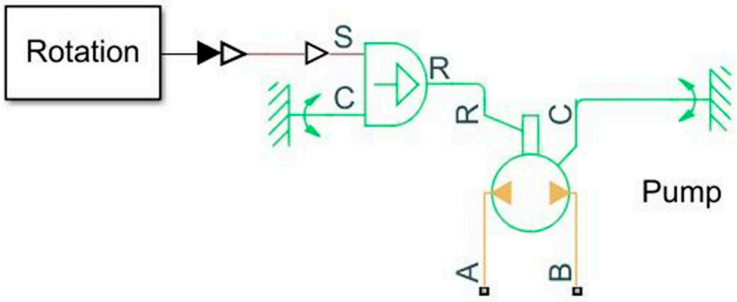


Figure 2. Fixed-displacement water pump module.

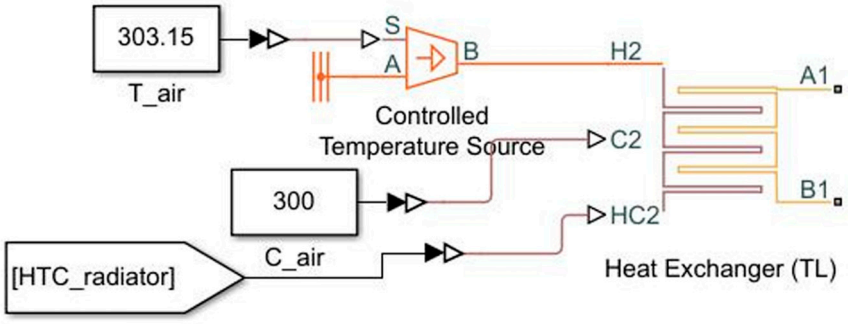


Figure 3. Heat transfer module.

A temperature-controlled valve module was used to simulate the thermostat, as shown in Figure 5. A threshold was set for this module; when the working fluid temperature in the system exceeds the threshold, the module opens, connecting the modules at both ends.

In addition to the aforementioned modules, the pipe module is also one of the main components of the system, as shown in Figure 6. To simplify calculations, all pipe modules used in this study were set as adiabatic pipes, neglecting heat dissipation during the flow of cooling water.

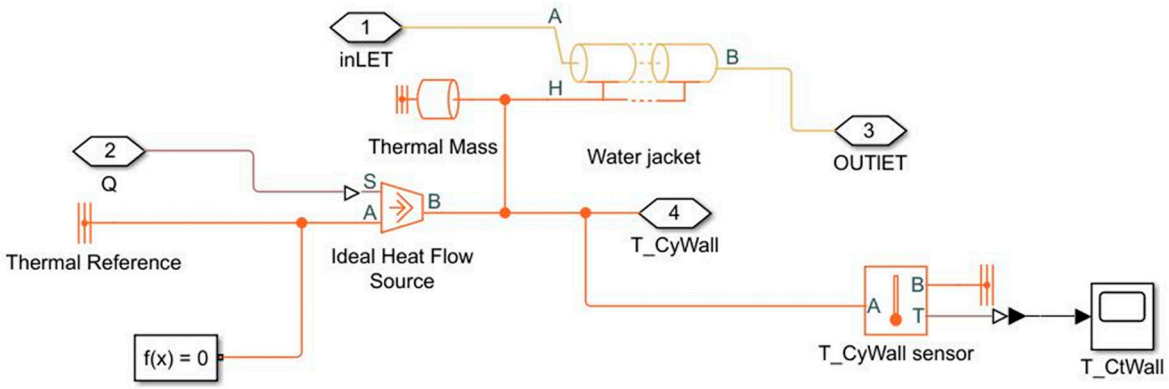


Figure 4. Engine module.

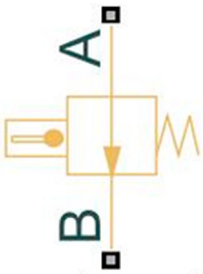


Figure 5. Temperature controlling valve module.

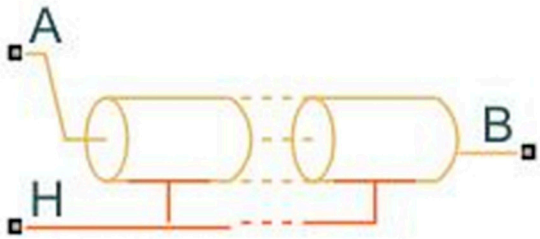


Figure 6. Pipe module.

Several output modules were set up for the model. The outputs of these modules include:

(1) The heat transfer coefficient input port HTC_radiator between the radiator pipe outer wall and air.
(2) The radiator inlet temperature output port radiator_inlet_Temperature.
(3) The engine inlet temperature output port engine_inlet_Temperature.
(4) The cylinder wall temperature output port cylinder_wall_Temperature.

It is worth noting that to simplify the modeling process and enhance computational efficiency, the one-dimensional Simulink simulation model established in this study is based on the following key assumptions:

(1) Adiabatic pipe assumption: All pipe modules are set to adiabatic conditions, ignoring the heat exchange between the coolant and the surrounding environment during its flow. This assumption may to some extent overestimate the thermal retention capacity of the system, especially under high-temperature or long pipeline conditions.
(2) Centralized parameter engine model: The engine module adopts the centralized parameter modeling method, that is, the engine water jacket is regarded as a uniform heat capacity body, without considering the local temperature gradients inside components such as the cylinder head and cylinder liner. This simplification is applicable to system-level thermal balance analysis, but it is insufficient to capture the details of local overheating or thermal stress distribution.

(3) Local representative radiator model: The radiator model only selects a single representative pipe for simulation and does not take into account the complex structural effects such as multiple pipes in parallel and uneven airflow distribution in actual radiators. This assumption helps to reduce the computational cost of three-dimensional CFD, but it may affect the prediction accuracy of the overall performance of the heat sink.

(4) Constant physical property coolant assumption: In the model, it is assumed that the thermal physical properties of the coolant, such as density, specific heat capacity, and thermal conductivity, do not change with temperature. In actual systems, the physical properties of the coolant changing with temperature may affect the flow and heat transfer characteristics, especially under high-temperature or large temperature difference conditions.

3. CFD Model

3.1. Radiator Model

This study employed Ansys Fluent as the fluid–thermal interaction (FTI) simulation tool. Since the convective heat transfer coefficient of the radiator pipes is closely related to air flow velocity and coolant flow velocity, a 3D model of the radiator was established for numerical simulation. To simplify calculations, a local heat exchanger pipe model was selected as the research object, as the actual heat exchanger consists of multiple long pipes. To enhance heat transfer efficiency, the fins in the model were angled upward. The meshed model is shown in Figure 7. To simulate the heat exchange process between air and the radiator surface, a rectangular prism representing the air domain was created around the model, with defined inlet and outlet boundaries to simulate air flow.

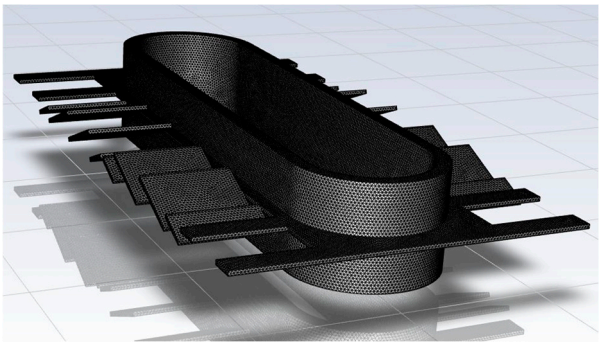


Figure 7. Mesh generation for the radiator pipes.

The inlet velocity of the air domain affects the convective heat transfer coefficient on the outer wall of the radiator. Therefore, the inlet velocity must be set according to the fan speed under different operating conditions. The air_inlet boundary type was set as a velocity inlet, with the inlet velocity adjusted based on fan speed and the inlet temperature set to 300 K. Since the pressure and velocity at the radiator air domain outlet are unknown and unconstrained, the air_outlet boundary type was set as a pressure outlet. The faces_air surface represents the interface between the radiator model and the external environment. The heat transfer mode on this surface was set to Mixed, with an incoming flow temperature of 300 K and a heat transfer coefficient of 20 W/(m^2·K), simulating natural convection between the external air and the air domain. The external radiation temperature was also set to 300 K. The faces_fin surface represents the inner wall of the radiator in contact with high-temperature coolant. The heat transfer mode on this surface was set to Mixed, with the incoming flow temperature determined by the Simulink model simulation results for the radiator inlet temperature at different times. Calibration was carried out by referring to the measured data of the diesel engine water jacket in the study by Xiao et al. [14], and

in combination with the typical convective heat transfer coefficient range of the coolant and the aluminum radiator in the built-in material library of FLUENT. The heat transfer coefficient was empirically set to 1200 W/(m^2·K).

3.2. Engine Model

In this study, the engine model consists of the cylinder head, cylinder liner, and cooling water sections. The overall mesh diagram of the model is shown in Figure 8, and the geometric models of each section are shown in Figure 9a–c. Volume meshes were generated based on these regions.

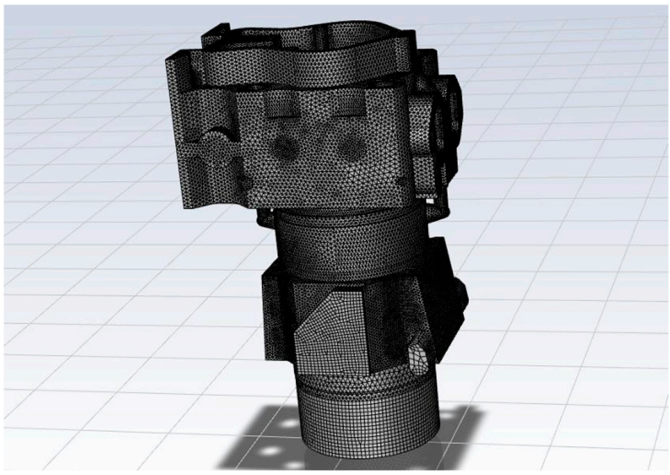
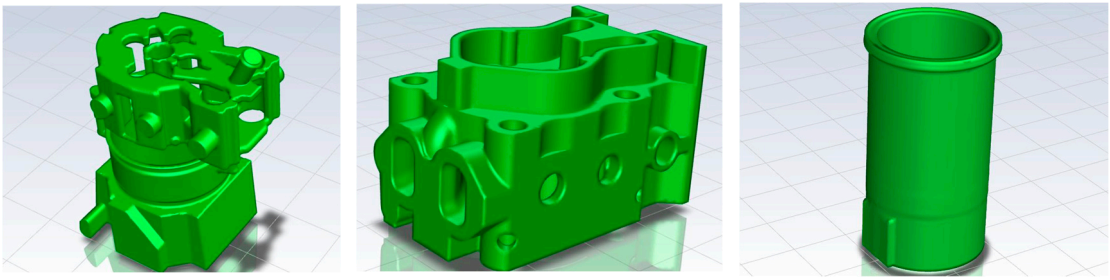


Figure 8. Mesh generation of engine.



(**a**) (**b**) (**c**)

Figure 9. Cooling water (**a**), head (**b**) and cylinder liner (**c**) model.

The cooling water section was defined as the liquid domain, with its inlet face mesh set as a velocity inlet to reflect different water pump speeds. The boundaries between the cooling water and the cylinder liner/head were set for convective heat transfer, using a coupled heat transfer type, with the convective heat transfer coefficient derived from the fluid–thermal interaction (FTI) method. The cylinder head and liner sections were defined as solid domains, with their face meshes set as walls and the heat transfer mode set to Mixed.

To define the grid size, we conducted a study on the verification of grid independence. Four different specifications of basic grid sizes were set, and the average temperature results of the cylinder liner in the three-dimensional simulation were analyzed as shown in Table 1. By comparison, it can be seen that before the grid size drops to 3 mm, there is still a significant difference in the average temperature results. However, the difference between the results corresponding to the base size of 3 mm and 2.5 mm is already small enough. Therefore, 3 mm is chosen as the base grid size.

Table 1. Verification results of mesh independence.

Sample Number	Base Grid Size	T_{avg}/K
1	5 mm	385.5215
2	4 mm	384.8741
3	3 mm	384.5621
4	2.5 mm	384.3252

To reflect the actual operating conditions of the engine, the intake and exhaust passages in the cylinder head model were set for convective heat transfer. The incoming gas temperatures were set to 300 K and 673 K, respectively.

3.3. The Co-Simulation Method Integrates CFD with the Simulink Model

While the aforementioned 1D Simulink model systematically describes the temperature changes in the cooling system, it neglects the variations in convective heat transfer coefficients due to changes in coolant and air flow rates. Therefore, this study utilizes CFD 3D simulation results to provide real-time updates of convective heat transfer coefficients to the Simulink model, while using the water temperatures obtained from Simulink simulations as initial conditions for the CFD simulations. The overall co-simulation process is illustrated in Figure 10. A specific time step is selected, and at each time node, the 1D and 3D results are exchanged. This process is accomplished by writing TUI (Text User Interface) commands in MATLAB that are recognizable by Fluent. The step size of the one-dimensional/three-dimensional simulation coupling is 1 s, and the total simulation duration is 500 s to ensure the stability of the results.

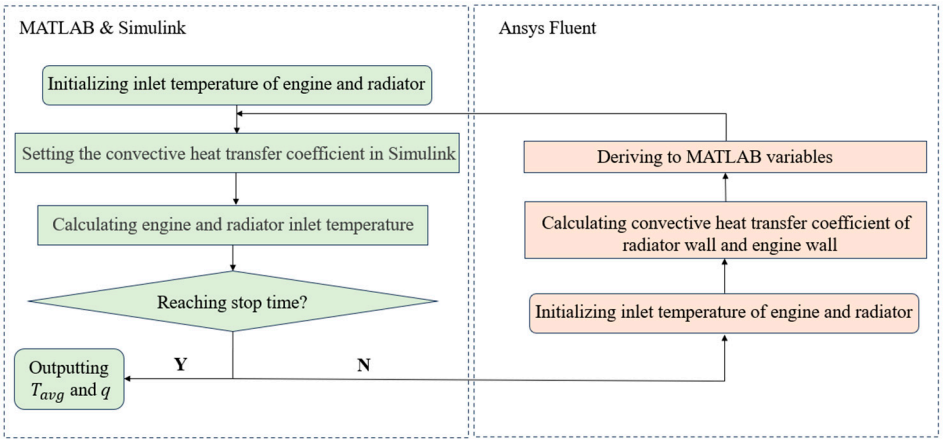


Figure 10. Co-simulation methodology of 1D and 3D simulation.

4. Optimization of Cooling Water and Air Flow Rates

4.1. Decision Variables and Optimization Objectives

As mentioned earlier, adjusting the coolant flow rate and air flow rate (corresponding to the speeds of the electric water pump and fan) can enhance cooling performance but may also reduce the engine's effective thermal efficiency. Therefore, it is necessary to optimize the flow rates of the cooling medium. This study employs NSGA-II (Non-dominated Sorting Genetic Algorithm II) as the tool to solve this multi-objective optimization problem.

The coolant flow rate and air flow rate were selected as decision variables for optimization, while the engine heat dissipation q and the average cylinder liner temperature T_{avg} were chosen as optimization objectives, representing the impact on thermal efficiency and cooling performance, respectively. Using Latin Hypercube Sampling, 25 different combinations of decision variables for the optimization algorithm were obtained, as listed

in Table 2. The coolant flow rate was constrained to the range of 2–4 m/s, and the air flow rate was constrained to the range of 4–12 m/s.

Table 2. Combination of decision variables for optimization.

Sample Number	Cooling Water Velocity/(m·s^{-1})	Air Velocity/(m·s^{-1})
1	2.83	9.05
2	3.66	9.36
3	3.69	6.92
4	3.20	7.08
5	2.18	8.05
6	2.27	10.29
7	2.24	11.30
8	2.01	10.45
9	2.10	7.23
10	3.17	10.69
11	3.79	5.28
12	2.59	4.46
13	2.65	4.56
14	3.88	5.71
15	3.81	6.27
16	3.35	5.97
17	4.00	4.05
18	2.47	8.66
19	3.28	5.01
20	2.40	5.48
21	2.44	10.02
22	3.42	10.94
23	2.75	11.57
24	2.72	9.68
25	2.83	11.81

4.2. Mathematical Model

Using NSGA-II to solve the aforementioned optimization problem essentially involves optimizing the nonlinear relationship between the decision variables and the optimization objectives, i.e.,

$$T_{avg} = f_1\left(n_w, n_f\right) \tag{1}$$

$$q = f_2\left(n_w, n_f\right) \tag{2}$$

where n_w and n_f represent the flow rates of the coolant and air, respectively.

To ensure the cylinder liner temperature does not exceed the material's melting point, a temperature threshold T_m is defined. Additionally, since the heat dissipation of the coolant cannot exceed the engine power, a threshold of heat density P_e is set. The constraints are expressed as:

$$g_1(x) = f_1\left(n_w, n_f\right) - T_m \leq 0 \tag{3}$$

$$g_2(x) = f_2\left(n_w, n_f\right) - P_e \leq 0 \tag{4}$$

5. Results and Discussions

5.1. Simulink Simulation Results

To evaluate the effectiveness of the Simulink 1D model and validate the impact of the radiator heat transfer coefficient on water temperature changes, preliminary observations

of the engine inlet coolant temperature were conducted under engine power conditions of 50 kW and 65 kW. The results are shown in Figures 11a and 11b, respectively.

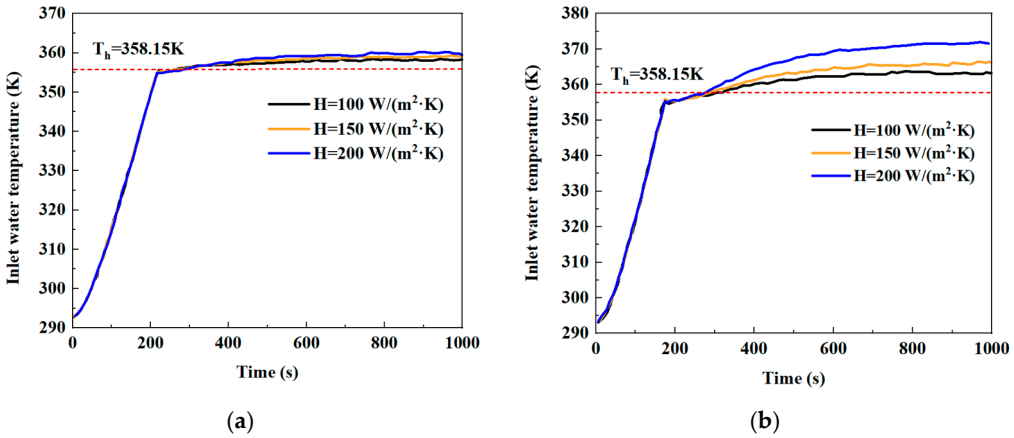


Figure 11. Engine inlet coolant temperature at engine power levels of 50 kW (**a**) and 65 kW (**b**).

The engine inlet coolant temperature initially exhibits a rapid rise. This is because the thermostat has not yet opened, and the coolant has not begun to function effectively. When the water temperature reaches the thermostat's threshold, the rate of temperature increase gradually slows and eventually stabilizes. As the heat transfer coefficient increases, the final coolant temperature decreases, indicating enhanced cooling performance. With higher engine power, the overall coolant temperature increases to some extent.

The inflection point in the temperature curve corresponds to the opening moment of the thermostat. In the initial stage, the thermostat is turned off, and the coolant only circulates inside the engine, causing the temperature to rise rapidly. When the coolant temperature reaches the thermostat threshold (approximately 85 °C), the thermostat opens, and the coolant begins to flow through the radiator for heat dissipation, resulting in a significant slowdown in the temperature rise rate and eventually stabilizing.

5.2. CFD Simulation Results

Figure 12a,b show the cylinder liner temperature distributions at coolant flow rates of 2 m/s and 4 m/s, respectively. Due to the flow of coolant outside the cylinder liner, the temperature is significantly lower than that of the interior. The average temperatures T_{avg} for the two cases are 376.6 K and 373.8 K, respectively, indicating that increasing the coolant flow rate enhances heat transfer capability.

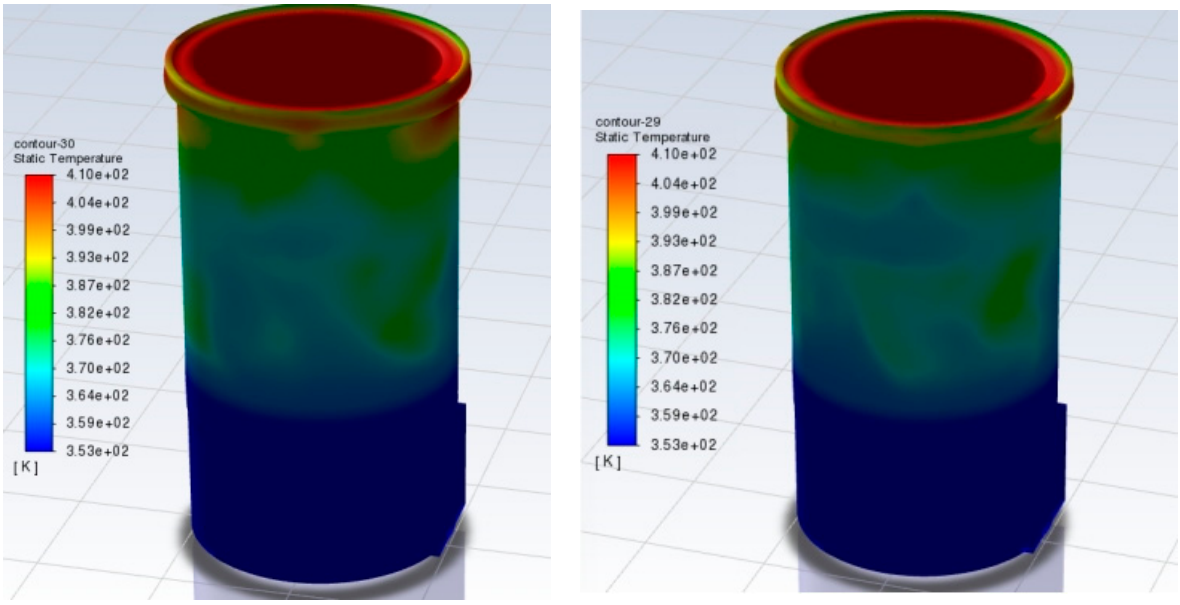
Co-simulations were performed for the 25 sampled combinations of decision variables, and the average cylinder liner temperatures and heat dissipation values were obtained through CFD, as shown in Tables 2 and 3.

Using the least squares method for polynomial fitting on the results from Tables 3 and 4, the mathematical relationships between the optimization objectives and the decision variables were derived, as shown in Equations (5) and (6).

$$T_{avg} = 423.70 - 14.67n_w - 2.028n_f + 1.582n_w^2 + 0.0921n_f^2 - 0.063n_f \cdot n_w \quad (5)$$

$$q = 85960 + 738.4n_w - 8.980n_f - 111.4n_w^2 + 6.505n_f^2 - 0.079n_f \cdot n_w \quad (6)$$

It is worth noting that the optimization objective function based on the fitting formula may have certain errors, which might be caused by the failure to consider the delays of each electronic component. In the future, an adaptive weight mechanism can be considered to address the reliance on human experience.



(**a**) (**b**)

Figure 12. Average cylinder liner temperature at coolant flow rates of 2 m/s (**a**) and 4 m/s (**b**).

Table 3. Simulation results of the average cylinder liner temperature.

Air Velocity/(m·s^{-1})	Cooling Water Velocity/(m·s^{-1})	T_{avg}/K
9.05	2.83	382.1387
9.36	3.66	378.2572
6.92	3.69	379.7026
7.08	3.20	381.4258
8.05	2.18	387.8376
10.29	2.27	385.9739
11.30	2.24	385.8097
10.45	2.01	388.5564
7.23	2.10	389.0342
10.69	3.17	379.9789
5.28	3.79	381.0896
4.46	2.59	388.3217
4.56	2.65	387.8401
5.71	3.88	380.3065
6.27	3.81	379.8428
5.97	3.35	381.9045
4.05	4.00	382.7691
8.66	3.54	379.2146
5.01	2.47	388.0129
5.48	3.28	384.4331
10.02	2.40	385.0322
10.94	2.44	384.1317
11.57	3.42	378.4553
9.68	2.75	382.6413
11.81	2.72	382.0806

Table 4. Simulation results of the average heat dissipation on the outer wall of the cylinder liner.

Air Velocity/(m·s^{-1})	Cooling Water Velocity/(m·s^{-1})	q/(W·m^{-2})
9.05	2.83	87,192.22
9.36	3.66	87,295.72
6.92	3.69	87,322.72
7.08	3.20	87,225.13
8.05	2.18	87,095.53
10.29	2.27	87,123.08
11.30	2.24	87,102.79
10.45	2.01	87,071.99
7.23	2.10	87,046.00
10.69	3.17	87,376.76
5.28	3.79	87,252.67
4.46	2.59	87,187.99
4.56	2.65	87,191.74
5.71	3.88	87,239.36
6.27	3.81	87,223.82
5.97	3.35	87,330.95
4.05	4.00	87,184.15
8.66	3.54	87,288.03
5.01	2.47	87,087.96
5.48	3.28	87,206.70
10.02	2.40	87,170.56
10.94	2.44	87,160.095
11.57	3.42	87,327.06
9.68	2.75	87,264.97
11.81	2.72	87,246.99

5.3. NSGA-II Optimization Results

From the aforementioned results, it is evident that under different combinations of coolant flow rate and air flow rate, the thermal load on critical engine components and the heat dissipation of the coolant are optimization objectives that exhibit opposing trends. This study combines Equations (1)–(6) and employs NSGA-II to solve the multi-objective optimization problem of the electronic cooling system. The Pareto frontier of the decision variables is shown in Figure 13. The results in the figure are mutually non-dominated. The discontinuity in the middle section arises because the T_{avg} values on the left side are consistently better than those on the right, while their q values are similar, resulting in a dominance relationship.

To investigate the differences in results under varying emphasis on optimization objectives, this study set three different weight configurations during the optimization process. The results are shown in Table 5. Comparing the optimization results under the three weight configurations reveals that the coolant flow rate has a significant influence on the changes in the optimization objectives. Specifically, a higher coolant flow rate tends to minimize both optimization objectives. For the air flow rate, increasing the air flow rate over the radiator surface shifts the optimal solution toward a lower average cylinder liner temperature, while reducing the air flow rate shifts the optimal solution toward lower heat dissipation from the cylinder liner.

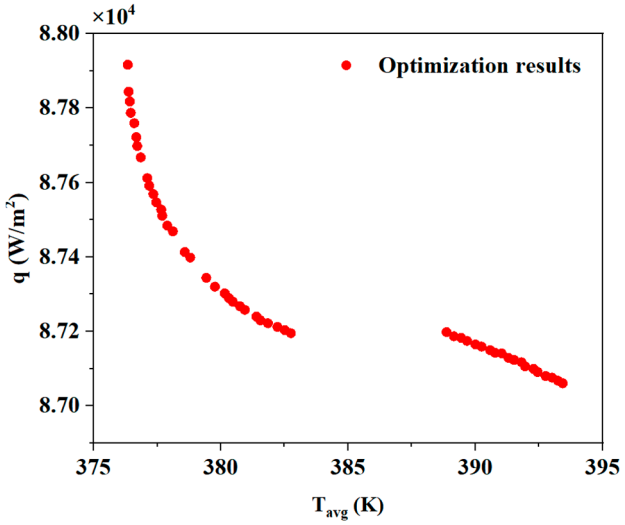


Figure 13. Pareto frontier of T_{avg} and q.

Table 5. Optimal decision variable combinations under different weightings of T_{avg} and q.

Weights	Air Velocity/(m·s^{-1})	Cooling Water Velocity/(m·s^{-1})
1:1	9.59	4
4:1	11.53	4
1:4	5.88	4

6. Conclusions

(1) A 1D simulation model of a powertrain electronic cooling system was established using Simulink, and the engine coolant inlet temperature was observed under varying heat transfer coefficients and engine power conditions.

(2) Numerical studies on the average cylinder liner temperature and heat dissipation were conducted using a CFD model of the engine cooling system. The average heat dissipation on the outer wall of the cylinder liner generally increased with higher coolant and air flow rates, with coolant flow rate having a more significant impact on heat dissipation.

(3) A 1D/3D co-simulation method for powertrain cooling systems was developed. After sampling coolant and air flow rates, co-simulations were performed, yielding 25 sets of data for average cylinder liner temperature (T_{avg}) and average heat dissipation (q). Mathematical relationships between T_{avg}, q, and the two variables were derived using the least squares method.

(4) A multi-objective optimization model for the cooling system was established, with coolant flow rate and air flow rate as decision variables, and average cylinder liner temperature (T_{avg}) and heat dissipation (q) as optimization objectives. NSGA-II was employed to complete the optimization process under different weight configurations, providing a methodological reference for the development of electronic cooling systems.

(5) The collaborative simulation and intelligent optimization framework proposed in this research institute has certain scalability and application prospects. In the future, it can be further applied to the design of thermal management systems for hybrid and pure electric vehicles, and the combination with adaptive control methods such as reinforcement learning can be explored to achieve real-time energy management under dynamic working conditions. Through bench tests to verify the integration with multiple cooling loops, phase change materials and other technologies, this research

is expected to provide a systematic solution for the intelligent thermal management of the next generation of high-power-density power systems.

Author Contributions: Conceptualization, J.Z.; methodology, F.Z.; software, X.S.; validation, X.S.; investigation, J.Z. and X.S.; data curation, W.Y. and F.Z.; writing—original draft, J.Z. and X.S.; writing—review & editing, W.Y. and F.Z.; visualization, X.S.; supervision, J.Z., W.Y. and F.Z.; project administration, W.Y. All authors have read and agreed to the published version of the manuscript.

Funding: The authors greatly acknowledge the support of National Key R&D Program of China (No. 2021YFD2000302).

Data Availability Statement: The data that support the findings of this study are available from the corresponding author upon reasonable request.

Conflicts of Interest: Author Jiwei Zhang was employed by the Weichai Lovol Intelligent Agricultural Technology Co, Ltd. The remaining authors declare that the research was conducted in the absence of any commercial or financial relationships that could be construed as a potential conflict of interest.

References

1. Hingne, M.; Dwivedi, R.; Choudri, R.V.; Chhalotre, S. Analysing the effect of weight reduction of Crankshaft on the pressure parameter inside cylinder of single cylinder SI engine. *Mater. Today Proc.* **2021**, *47*, 6296–6300. [CrossRef]
2. Liu, Y.; Lei, J.; Chen, J.; Wen, J.; Jiang, X.; Peng, H. Research on lightweight design method of diesel engine steel piston based on heat transfer characteristics. *Appl. Therm. Eng.* **2024**, *248*, 123344. [CrossRef]
3. Cipollone, R.; Di Battista, D. *Performances and Opportunities of an Engine Cooling System with a Double Circuit at Two Temperature Levels*; SAE International: Warrendale, PA, USA, 2012.
4. Lu, P.; Gao, Q.; Wang, Y. The simulation methods based on 1D/3D collaborative computing for the vehicle integrated thermal management. *Appl. Therm. Energy* **2016**, *104*, 42–53. [CrossRef]
5. Haghighat, A.K.; Roumi, S.; Madani, N.; Bahmanpour, D.; Olsen, M.G. An intelligent cooling system and control model for improved engine thermal management. *Appl. Therm. Eng.* **2018**, *128*, 253–263. [CrossRef]
6. Ap, N.-S.; Tarquis, M. *Innovative Engine Cooling Systems Comparison*; SAE International: Warrendale, PA, USA, 2005.
7. Melling Tool Co. Temperature Control Apparatus and Method For an Powertrain Cooling System. U.S. Patent 10,060,328, 27 August 2013.
8. Cortona, E.; Onder, C.H. *Engine Thermal Management with Electric Cooling Pump*; SAE International: Warrendale, PA, USA, 2000.
9. Osman, K.A.; Higginson, A.M.; Moore, J. Improving the efficiency of vehicle water-pump designs using genetic algorithms. In *Smart Engineering Systems: Proceedings of the Artificial Neural Networks in Engineering Conference*; ASME Press: New York, NY, USA, 1998; pp. 291–296.
10. Wagner, J.R.; Srinivasan, V.; Dawson, D.M.; Marotta, E.E. *Smart Thermostat and Coolant Pump Control for Engine Thermal Management Systems*; SAE Special Publication: Warrendale, PA, USA, 2003.
11. Wang, Y.; Bi, A.; Yao, Y.; Chen, W.; Chen, K.; Yu, S.; Yu, J.; Wang, C.; Li, W.; Wang, S. Thermal analysis and multi-objective optimization of equal-area microfluidic cooling systems. *Results Eng.* **2025**, *27*, 105869. [CrossRef]
12. Amiri-Margavi, A.; Jamali, R.; Hosseini, S.A.; Torabi, F. Real-time optimization of thermoelectric coolers' performance based on energy and exergy analysis. *arXiv* **2024**, arXiv:2403.01614. [CrossRef]
13. Paneer, M.; Bašić, J.; Sedlar, D.; Lozina, Ž.; Degiuli, N.; Peng, C. Fluid Structure Interaction Using Modal Superposition and Lagrangian CFD. *J. Mar. Sci. Eng.* **2024**, *12*, 318. [CrossRef]
14. Zhu, W.; Lin, W.; Zhang, S.; Yang, S.; Wu, T.; Ma, R.; Cao, T.-F.; Dai, Y.-J.; Tao, W.-Q. Modeling and analysis of fluid-solid coupling heat transfer and fluid flow in transonic nozzle. *Appl. Therm. Eng.* **2025**, *260*, 124885. [CrossRef]
15. Schäfer, M.; Teschauer, I. Numerical simulation of coupled fluid–solid problems. *Comput. Methods Appl. Mech. Eng.* **2001**, *190*, 3645–3667. [CrossRef]
16. Chen, H.Y.; Li, Y.; Li, X.L. Simulation study on the fluid-solid coupled heat transfer of diesel engines. *J. China Jiliang Univ.* **2006**, *17*, 284–288.
17. Nageswara, R.; Sukhvinder, K.; Ravi, K.; Niranjan, K. *CFD Analysis of Axial Flow Fans for Radiator Cooling in Automobile Engines*; SAE International: Warrendale, PA, USA, 2007.
18. Zeng, Z.; Yuan, N.; Song, C.; Liu, J.; Liu, Z.; Shi, H. Integrating CFD and data-driven techniques for the optimization of dielectric coolants in EV battery immersion cooling systems. *Int. Commun. Heat Mass Transf.* **2025**, *162*, 108591. [CrossRef]
19. Park, K.S.; Won, J.P.; Heo, H.S. Thermal flow analysis of vehicle engine cooling system. *KSME Int. J.* **2002**, *16*, 975–985. [CrossRef]

20. Adsul, P.; Kotebavi, V.; Bedekar, S.; Mishra, A. A Simulation study of cooling system for heavy duty diesel engine. *MATEC Web Conf.* **2018**, *172*, 02002. [CrossRef]
21. Qiu, S.; Xu, C.; Yang, Z.; He, H.; Xia, E.; Xue, Z.; Li, L. One-dimension and three-dimension collaborative simulation study of the influence of non-uniform inlet airflow on the heat transfer performance of automobile radiators. *Appl. Therm. Eng.* **2021**, *196*, 117319. [CrossRef]
22. Holland, J.H. *Adaption in Natural and Artificial Systems*; University of Michigan Press: Ann Arbor, MI, USA, 1975; pp. 126–137.
23. Wang, Z.; Tingxu, L.; Yongkang, S. Optimization of the maximum range of super cavitating vehicles based on a genetic algorithm. *Ocean Eng.* **2021**, *239*, 109892.
24. Soundar, K.; Inyong, H. Use of Associative Memory and Self-Organization in Conceptual Design. *CIRPAnnals* **1990**, *39*, 117–120.
25. Srinivas, N.; Deb, K. Multi objective Optimization Using Nondominated Sorting in Genetic Algorithms. *Evol. Comput.* **1994**, *2*, 221–248. [CrossRef]
26. Deb, K.; Pratap, A.; Agarwal, S.; Meyarivan, T. A fast and elitist multiobjective genetic algorithm: NSGA-II. *IEEE Trans. Evol. Comput.* **2002**, *6*, 182–197. [CrossRef]
27. Deb, K.; Jain, H. An Evolutionary Many-Objective Optimization Algorithm Using Reference-Point-Based Nondominated Sorting Approach, Part I: Solving Problems with Box Constraints. *IEEE Trans. Evol. Comput.* **2014**, *18*, 577–601. [CrossRef]
28. Li, H.P.; Figliola, R.S. *Optimization of an Powertrain Cooling System Based on Exergy Analysis*; SAE International: Warrendale, PA, USA, 2004.

Disclaimer/Publisher's Note: The statements, opinions and data contained in all publications are solely those of the individual author(s) and contributor(s) and not of MDPI and/or the editor(s). MDPI and/or the editor(s) disclaim responsibility for any injury to people or property resulting from any ideas, methods, instructions or products referred to in the content.